

Stress/Displacement Field Calculation for Bolted Joint Based on State Space Theory

*Q.C. Sun**, *Y.J. Jiang*, *X. Huang*, *W.Q. Huang*, *Z.Y. Sun*, *X.K. Mu*

School of Mechanical Engineering, Dalian University of Technology, China

*Corresponding author: sqc_dut@163.com

Abstract.

Stress/displacement field analyzing of mechanical assembly is important for predicting mechanical property, and optimizing structural parameters and assembly technology parameters of mechanical assembly. However the structural discontinuity and material difference of mechanical assembly determines the complexity of stress function, it is difficult for analytically computing stress/displacement field of mechanical assembly. In this paper, taking bolted joint under the action of normal load as the research object, a stress/displacement field layered mapping and calculating model of mechanical assembly is proposed, with considering the stress/displacement transmission characteristics of mechanical assembly, combining state space method and elastic mechanics theory. The model divides mechanical assembly as the layered structures, and determines layered constraint conditions according to structural discontinuity or continuity in different positions, such as the structure at the junction surfaces is discontinuous. Considering the difference between bolted joint and the common axisymmetric structure, taking the stresses σ_z , τ_{zr} and the displacements u , w as the state variables, the state equations based on Fourier-Bessel series was built to express the stress/displacement transmission relationships. Linearizing the stress/displacement transmission rules, the relationships between state variables at arbitrary and external load were determined by accumulated calculating, and stress/displacement characteristics at arbitrary positions of bolted joint structure were obtained. Finally, the pressure distribution of the bolted joint interface, and stress/displacement distribution of the whole bolted joint structure was calculated, the comparison among the analytically calculation, FEA and the test data proves the effectiveness of the model.

Keywords: Structural discontinuity, Bolted joint, Stress/displacement field, State space method, Elastic mechanics

1. Introduction

Mechanical systems are usually composed of multiple parts, which were assembled according to the specific requirements. The contact surfaces among these parts are known as the "joint surfaces" or "interfaces", such as bolted joint surfaces, guide contact surfaces and the mating surface between hole and shaft. The joint surfaces, together with the influence area of stress/deformation in the connected mechanical components, are known as "joint" [1].

Joint surfaces / joints have remarkable influence on the statics, dynamics and thermodynamic characteristics of mechanical systems, and obtaining the stress / displacement distribution in joints is the basis for accurately analyzing the characteristics of mechanical systems. Joint surfaces / joints stiffness, which is closely related to the stress / displacement distribution in the joints, is a key factor affecting the accuracy of the mechanical systems [2, 3]. Bolted joints and hole-shaft mating surfaces often occur fretting fatigue under the external alternating loads, which leads to premature parts failure, and the stress / displacement distribution in joints is the main factor affecting fretting fatigue [4]. The dynamics characteristics are the key

features of mechanical assemblies, the stiffness distributions in joints are the important factors influencing dynamics characteristics, and obtaining the stress / displacement fields is the premise of calculating stiffness of joints and revealing the dynamics of assemblies [5-7]. Moreover, determining the contact area distribution and elastic-plastic contact state in joints have also great significance for analyzing heat transfer mechanism of assemblies [8, 9]. However, it is difficult to measure directly the stress/displacement distribution in joints, theoretical analysis and calculation are the primary means of obtaining stress / displacement fields information.

Compared to a single part, the structural discontinuity and material difference of mechanical assemblies makes it difficult to calculate the stress / displacement field based on the traditional elasticity theory. The traditional elasticity theory based on the continuity, uniformity and other basic assumptions, and one component is composed of the same material, the stress, deformation and displacement characteristics in one component are completely continuous. The mechanical assemblies have the discontinuous structure characteristics, the stress /displacement distribution of joint surfaces is unknown. Because lacking mature stress/ displacement distribution function under the unknown boundary conditions[10-12], it is difficult to accurately calculate the stress/displacement field of the mechanical assembly in the traditional elastic mechanics system.

Finite element method (FEM) is the current main method of calculating the stress / displacement field in mechanical assembly [4, 6, 13-16]. The stress / displacement field calculation of joint surfaces / joints belongs to contact nonlinear problem, which requires large computation memory but embodies a low computational efficiency. Additionally, the FEM computation results depend on the high quality of grids, especially need dense grids in the contact area, which also limits the efficiency of solving such problems.

Combining with elastic mechanics, the state space methods have been used to calculate exactly the stress / displacement fields of laminated plates, functionally graded plates, and multi-layer civil structures, etc., these studies provide references for the stress/displacement field calculation of bolt joint. Such as, Xiang and Wang[17] obtained the exact buckling and vibration solutions of unidirectional ladder rectangular plates by combining the Levy method and the state space theory. Chen and Ding[18] derived two independent state equation with variable coefficients, and analyzed the freedom vibration of transversely isotropic piezoelectric material rectangular plate on the basis of three-dimensional theory equations of transversely isotropic piezoelectricity. Ying et al. [19] put forward the exact solutions of bending and free vibration for functionally graded beams placing on a Winkler–Pasternak elastic foundation, based on the two-dimensional elasticity theory and state space method. Adopting state space method, Hongyu and Jiarang [20, 21] obtained the analytical solutions of bending problem for clamped or simply supported thick laminated circular plate, as well as thick laminated circular plate on elastic foundation with free edges.

Taking the external load of joint surfaces/joints as the input information and stress/displacement distribution as the output information, and expressing the transmission characteristics of the stress/displacement as state transition matrix, the stress/displacement field can be calculated based on state space theory. The

stress/displacement field calculation of mechanical assemblies have the similar theory basis to the previous research objects[17-21], with discarding any assumptions about displacement pattern and stress distribution, and constructing the stress/displacement transfer matrix of mechanical assembly by adopting the state space differential equation.

The bolted joint under the action of normal load was selected as research object in this paper, the structure, material and loading mode of bolted joint are different from the laminated plates, etc., a new calculation model for bolted joint was built. And the traditional axial symmetry stress/displacement state equations do not completely match with the structural characteristics of bolted joint, the state equations for bolted joint was built.

2. State Space Method in Elastic Mechanics Problem

State space method is a method to analyze and synthesize control systems based on the state variable description in modern control theory. State space method describes the state of the system with the state variables, and establishes the relationship between the state variables within the system and the external input/output variable. State equation is the mathematical description which reflects the causal relationship between state variables and input variables in state space method. Because state space method uses matrix representation, the increase in the number of state variables, input variables or output variables, does not increase the complexity of the system description, which makes it especially suitable for dealing with multiple input, multiple output and multivariable system problems.

Using the state space method to solve the elastic mechanics problem, first of all, should select the key unknown variables as state variables, and then set up the mechanics model according to the actual problem. The number and the type of the state variables depend on the specific problem. For example, the stresses $\sigma_z, \tau_{xz}, \tau_{yz}$ and the displacements u, v, w can be selected as state variables, and constitute the state vector $S = [\sigma_z \quad \tau_{xz} \quad \tau_{yz} \quad u \quad v \quad w]^T$. The ordinary differential state equation of elastic mechanics problem can be obtained by physical equation, equilibrium equation, and a series of changes, such as series expansion, Laplace transform, Hankel transform, etc. Generally the form of ordinary differential state equation as follows:

$$\frac{d}{dz}S(z) = DS(z) + \tilde{\Phi}(z) \quad (1)$$

where $S(z)$ is the state vector, D is a square matrix related to material parameters, $\tilde{\Phi}(z)$ is an array related to boundary conditions. The state equation is obtained by solving **Eq. (1)** as follows:

$$S(z) = T(z)S(0) + \Phi(z) \quad (2)$$

where square matrix $T(z)$ is the state transition matrix. Thus, the state $S(z)$ that

transfers any distance along the z direction is obtained from **Eq. (2)**, with the known initial state $S(0)$.

The state space method is an effective way to deal with the discontinuous structure problem of mechanical joints, which divides the matching components into different "chains" and sets the boundary conditions so as to adapt to the material discontinuous characteristic in structure and material. And it calculate the stress/ displacement exactly by dividing a single component (corresponds to a "chain") into different virtual "layers". Moreover, the assembly that is divided into virtual layers, is an end-to-end chain system, whose state variables can be obtained from the simple accumulation of the state transition matrix. Since the number of the state variables don't vary with the number of "chains" or "layers", to a great extent, complex problems can be simplified.

3. Calculation Model for Bolted Joint

3.1 Model Assumption

To research the stress/displacement field in bolted joints, the analytical model is assumed to be the axisymmetric mechanics problem as shown in **Fig. 1**. The two bolted plates are expressed as hollow cylinder I and II with inner diameter $2a$ and outer diameter $2b$, whose thicknesses are h_1 and h_2 respectively. Preload is an axisymmetric distributed pressure $p(r)$ on the upper surface of hollow cylinder I over an annular region $a \leq r \leq c$. Hollow cylinder II corresponds to the bolted member with a fixed lower surface. All of the cylindrical surfaces of hollow cylinder I and II are free boundaries. Take the center of upper surface of hollow cylinder I as the coordinate origin O . Take the central axis of the hollow cylinders as the symmetry axis z , whose direction is vertical downward, and axis r is in the horizontal direction, the global cylindrical coordinate system (r, θ, z) is established as shown in **Fig. 1(a)**. in the same way, the local cylindrical coordinate systems (r, θ, z_1) and (r, θ, z_2) are established on hollow cylinder I and II, respectively.

To make the model as simple as possible, following basic assumptions are used:

- (1) The material of each hollow cylinder is assumed to be ideal elastic, continuous, homogeneous, and isotropic.
- (2) Body forces are ignored.
- (3) The roughness, flatness and other practical machining errors of the contact surface are ignored, the joint surface is absolutely smooth and flat.
- (4) The points in the contact surface of the two pieces of hollow cylinders always maintain contact during the loading process.

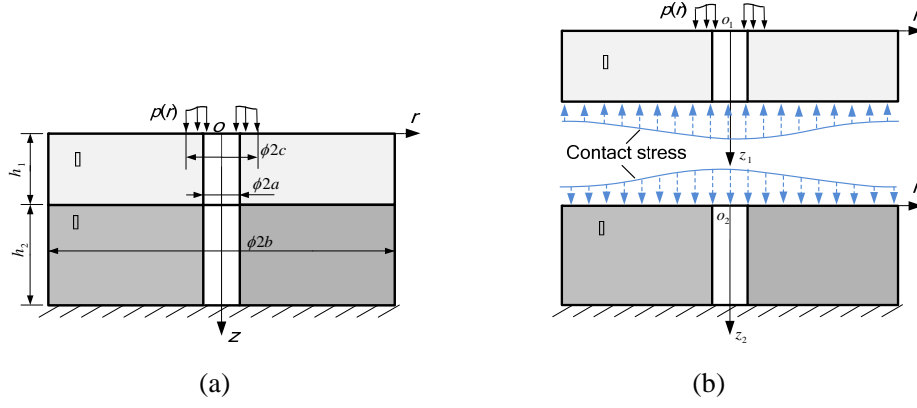


Fig. 1 Analytical model of bolted joint

3.2 Boundary Conditions

To simplify the calculation, the distributed pressure $p(r)$ in **Fig. 1** is assumed to be a uniformly distributed load whose resultant force is F :

$$p(r) = \begin{cases} p = \frac{F}{\pi(c^2 - a^2)} & (a \leq r \leq c) \\ 0 & (c < r \leq b) \end{cases} \quad (3)$$

In this paper, the superscripts (1) and (2) denote the mechanical characteristics of hollow cylinder I and II respectively, and u and w denote horizontal and vertical displacement respectively. The boundary conditions are given by **Eq. (4) ~ (7)**.

(1) The upper surface of hollow cylinder I :

$$z_1 = 0 : \sigma_z^{(1)} = -p(r), \tau_{zr}^{(1)} = 0, \quad (4)$$

(2) The lower surface of hollow cylinder II :

$$z_2 = h_2 : u^{(2)} = w^{(2)} = 0 \quad (5)$$

(3) The contact surface of hollow cylinder I and II :

$$z_1 = h_1, z_2 = 0 : \sigma_z^{(1)} = \sigma_z^{(2)}, w^{(1)} = w^{(2)}, \tau_{zr}^{(1)} = \tau_{zr}^{(2)} = 0 \quad (6)$$

(4) All of the cylindrical surfaces:

$$r = a, b : \tau_{zr}^{(1)} = \tau_{zr}^{(2)} = 0, \sigma_r^{(1)} = \sigma_r^{(2)} = 0 \quad (7)$$

3.3 State Equations

The stress/displacement field calculation in bolted joint under the normal load belongs to axisymmetric problem, whose physical equations are expressed as follows:

$$\begin{cases} \sigma_r = (\lambda + 2G) \frac{\partial u}{\partial r} + \lambda \frac{u}{r} + \lambda \frac{\partial w}{\partial z} \\ \sigma_\theta = \lambda \frac{\partial u}{\partial r} + (\lambda + 2G) \frac{u}{r} + \lambda \frac{\partial w}{\partial z} \\ \sigma_z = \lambda \frac{\partial u}{\partial r} + \lambda \frac{u}{r} + (\lambda + 2G) \frac{\partial w}{\partial z} \\ \tau_{rz} = G \left(\frac{\partial w}{\partial r} + \frac{\partial u}{\partial z} \right) \end{cases} \quad (8)$$

where λ is Lamé Constant, G is the shear modulus.

The equilibrium equations of axisymmetric problem are expressed as follows:

$$\begin{cases} \frac{\partial \sigma_r}{\partial r} + \frac{\partial \tau_{rz}}{\partial z} + \frac{\sigma_r - \sigma_\theta}{r} = 0 \\ \frac{\partial \tau_{rz}}{\partial r} + \frac{\partial \sigma_z}{\partial z} + \frac{\tau_{rz}}{r} = 0 \end{cases} \quad (9)$$

Let

$$\begin{aligned} C_1 &= -\frac{\lambda}{\lambda + 2G}, \quad C_2 = \lambda + 2G - \frac{\lambda^2}{\lambda + 2G} \\ C_3 &= \lambda - \frac{\lambda^2}{\lambda + 2G}, \quad C_4 = \frac{1}{\lambda + 2G}, \quad C_5 = \frac{1}{G} \end{aligned}$$

Eliminating σ_r and σ_θ from **Eq. (8)**, we obtain

$$\sigma_r = C_2 \frac{\partial u}{\partial r} + C_3 \frac{u}{r} - C_1 \sigma_z \quad (10)$$

$$\sigma_\theta = C_3 \frac{\partial u}{\partial r} + C_2 \frac{u}{r} - C_1 \sigma_z \quad (11)$$

Selecting u, w, τ_{rz} and σ_z as the state variables, the following is obtained from **Eq. (8)** and **(9)**.

$$\frac{\partial}{\partial z} \begin{Bmatrix} u \\ w \\ \tau_{zr} \\ \sigma_z \end{Bmatrix} = \begin{bmatrix} 0 & -\frac{\partial}{\partial r} & C_5 & 0 \\ C_1 \left(\frac{\partial}{\partial r} + \frac{1}{r} \right) & 0 & 0 & C_4 \\ C_2 \left(\frac{\partial^2}{\partial r^2} + \frac{1}{r} \frac{\partial}{\partial r} - \frac{1}{r^2} \right) & 0 & 0 & C_1 \frac{\partial}{\partial r} \\ 0 & 0 & -\left(\frac{\partial}{\partial r} + \frac{1}{r} \right) & 0 \end{bmatrix} \begin{Bmatrix} u \\ w \\ \tau_{zr} \\ \sigma_z \end{Bmatrix} \quad (12)$$

This paper expands the solution of **Eq. (9)** into following Fourier-Bessel series

$$\begin{cases} u(r, z) = \sum_{m=1}^{\infty} U_m(z) V_1(\alpha_m r) + r \tilde{U}(z) \\ w(r, z) = W_0(z) + \sum_{m=1}^{\infty} W_m(z) V_0(\alpha_m r) \\ \tau_{zr}(r, z) = \sum_{m=1}^{\infty} R_m(z) V_1(\alpha_m r) \\ \sigma_z(r, z) = Z_0(z) + \sum_{m=1}^{\infty} Z_m(z) V_0(\alpha_m r) \end{cases} \quad (13)$$

The form of Fourier - Bessel series Hongyu and Jiarang [20,21] proposed, can meet the boundary conditions of circular plate, but cannot meet the boundary conditions of bolted joint structure (hollow cylinder). To solve this problem, the form of the function $V_\mu(\alpha_m r)$ is structured as follows:

$$V_\mu(\alpha_m r) = J_\mu(\alpha_m r) - \frac{J_\mu(\alpha_m b)}{Y_\mu(\alpha_m b)} Y_\mu(\alpha_m r)$$

where $J_\mu(\alpha_m r)$ and $Y_\mu(\alpha_m r)$ are the first type and the second type μ -order Bessel functions separately. $\tilde{U}(z)$ is an unknown function for z . U_m, W_m, R_m and Z_m ($m=0,1,2,3,\dots$) are respectively the coefficients of Fourier-Bessel series of u, w, τ_{zr} and σ_z . $\alpha_m = \beta_m / a$, $\beta_m (m=1,2,3,\dots)$ is the m -th positive root satisfying the following equation

$$J_1(\beta_m) Y_1\left(\frac{b}{a} \beta_m\right) - J_1\left(\frac{b}{a} \beta_m\right) Y_1(\beta_m) = 0, \quad (0 < \beta_1 < \beta_2 < \beta_3 \dots) \quad (14)$$

$V_1(\alpha_m r)$ satisfies $V_1(\alpha_m a) = V_1(\alpha_m b) = 0$, therefore **Eq. (13)** satisfies the boundary conditions $\tau_{zr} = 0$ in **Eq. (7)**. In addition, to satisfy boundary conditions of cylindrical surfaces, there should be $\sigma_r = 0$ at $r = a$ or b . Substituting the first and the fourth equation of **Eq. (13)** into **Eq. (10)** and setting $\sigma_r = 0$, the following two equations can be obtained, and the unknown function $\tilde{U}(z)$ can be determined from **Eq. (15)** and **(16)**.

$$(C_3 + C_2)\tilde{U}(z) + \sum_{m=1}^{\infty} [C_2\alpha_m U_m(z) - C_1 Z_m(z)] V_0(\alpha_m a) - C_1 Z_0(z) = 0, \text{ at } r = a \quad (15)$$

$$(C_3 + C_2)\tilde{U}(z) + \sum_{m=1}^{\infty} [C_2\alpha_m U_m(z) - C_1 Z_m(z)] V_0(\alpha_m b) - C_1 Z_0(z) = 0, \text{ at } r = b \quad (16)$$

Performing the following series expansion

$$\begin{cases} r = \sum_{m=1}^{\infty} \tilde{A}_m V_1(\alpha_m r) \\ \left(\frac{\partial}{\partial r} + \frac{1}{r}\right)r = \tilde{B}_0 + \sum_{m=1}^{\infty} \tilde{B}_m V_0(\alpha_m r) \\ \left(\frac{\partial^2}{\partial r^2} + \frac{1}{r} \frac{\partial}{\partial r} - \frac{1}{r^2}\right)r = \sum_{m=1}^{\infty} \tilde{C}_m V_1(\alpha_m r) \end{cases} \quad (17)$$

The coefficients are obtained according to related knowledge of Fourier - Bessel series as follows

$$\begin{aligned} \tilde{A}_m &= \frac{c^2 V_2(\alpha_m c) - a^2 V_2(\alpha_m a)}{\alpha_m M_m} \\ \tilde{B}_0 &= 2 \\ \tilde{B}_m = \tilde{C}_m &= 0, (m = 1, 2, 3, \dots) \end{aligned}$$

Where

$$M_m = \frac{b^2 V_0^2(\alpha_m b) - a^2 V_0^2(\alpha_m a)}{2}$$

Substituting **Eq. (13)** and **(17)** into **Eq. (12)**, the following equation can be obtained

$$\frac{d}{dz} S(z) = DS(z) + \tilde{\Phi}(z) \quad (18)$$

Where

$$S(z) = [U_m(z) \quad W_m(z) \quad R_m(z) \quad Z_m(z)]^T \quad (19)$$

$$D = \begin{bmatrix} 0 & \alpha_m & C_5 & 0 \\ C_1 \alpha_m & 0 & 0 & C_4 \\ C_2 \alpha_m^2 & 0 & 0 & -C_1 \alpha_m \\ 0 & 0 & -\alpha_m & 0 \end{bmatrix} \quad (20)$$

$$\tilde{\Phi}(z) = \begin{bmatrix} -\tilde{A}_m \frac{d\tilde{U}(z)}{dz} & C_1 \tilde{B}_m \tilde{U}(z) & -C_2 \tilde{C}_m \tilde{U}(z) & 0 \end{bmatrix}^T \quad (21)$$

Eq. (17) is a nonhomogeneous ordinary differential equation, and solving it yields the state equation as follows

$$S(z) = T(z)S(0) + \Phi(z) \quad (22)$$

Where

$$T(z) = e^{Dz} \quad (23)$$

$$\Phi(z) = \int_0^z e^{D(z-t)} \tilde{\Phi}(t) dt \quad (24)$$

In **Eq. (22)**, $S(z)$ is the state vector at z , namely the coefficient terms of Fourier-Bessel series, $S(0)$ is the initial state vector on the upper surface. For a certain m , the matrix D is a constant matrix, so $T(z)$ can be obtained. The parameters of $\Phi(z)$ are known except $\tilde{U}(z)$. Therefore, For a certain m , the state vector $S(z)$, namely the coefficients of Fourier-Bessel series U_m , W_m , R_m and Z_m at z , can be obtained with the initial state vector $S(0)$ in **Eq. (22)**, only if the function $\tilde{U}(z)$ is determined.

Particularly, there are the following relation for $m = 0$.

$$\begin{cases} \frac{d}{dz} Z_0(z) = 0 \\ \frac{d}{dz} W_0(z) = C_4 Z_0(z) + C_1 \tilde{B}_0 \tilde{U}(z) \end{cases} \quad (25)$$

3.4 Coefficients of Fourier-Bessel Series for $m \geq 1$

Determining the function $\tilde{U}(z)$ is the key to Stress/displacement field calculation. As shown in **Fig. 2**, the j -th hollow cylinder is divided into N_j virtual sublayers averagely, and the thickness of each sublayer is $d_j = h_j / N_j$. Let $x_{j,i}$ and $x_{j,i+1}$ be the end-values of the upper surface and the lower surface of the i -th sublayer in the j -th hollow cylinder, respectively. As shown in **Fig. 3**, provided that the sublayer is

thin enough, it is reasonable to consider that the unknown function $\tilde{U}(z)$ in the sublayer is linear distributed along z direction [20]. So in the i -th sublayer of the j -th hollow cylinder, function $\tilde{U}(z)$ can be denoted by $\tilde{U}_{j,i}(z_{j,i})$ as follows, in the local coordinate system whose origin of axis $z_{j,i}$ is on the upper surface of the sublayer.

$$\tilde{U}_{j,i}(z_{j,i}) = \frac{x_{j,i+1} - x_{j,i}}{d_j} \cdot z_{j,i} + x_{j,i}, \quad (0 \leq z_{j,i} \leq d_j, i=1,2,\dots,N_j, j=1,2) \quad (26)$$

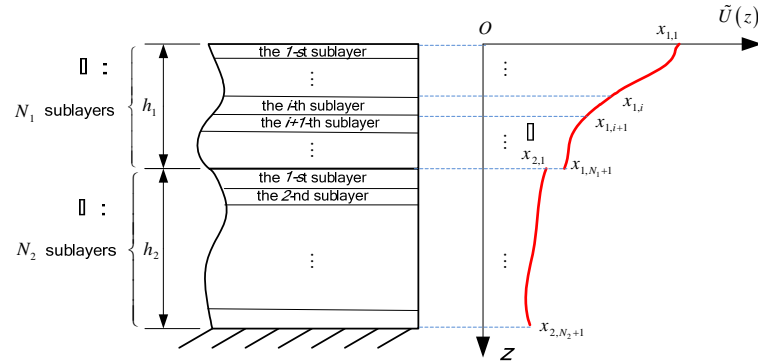


Fig. 2 Sublayers and corresponding $\tilde{U}(z)$

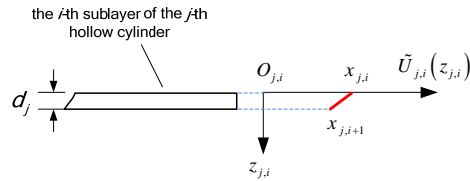


Fig. 3 Linear distribution assumption

Linear distribution assumption (26) causes calculation error, but if the number of the sublayers N_j increases gradually, the error will decrease. So the error is controllable and N_j can be determined based on the accuracy requirement. For any sublayer, the ordinary differential state equation is obtained according to **Eq. (18), (21) and (26)**

$$\frac{d}{dz} S_{j,i}(z_{j,i}) = D_j S_{j,i}(z_{j,i}) + \tilde{\Phi}_{j,i}(z_{j,i}) \quad (27)$$

Where

$$\tilde{\Phi}_{j,i}(z_{j,i}) = \begin{bmatrix} \tilde{A}_m \frac{x_{j,i} - x_{j,i+1}}{d_j} & 0 & 0 & 0 \end{bmatrix}^T \quad (28)$$

According to **Eq. (22) ~ (24)**, the solution of **Eq. (27)** is obtained

$$S_{j,i}(z_{j,i}) = T_j(z_{j,i})S_{j,i}(0) + \Phi_{j,i}(z_{j,i}) \quad (29)$$

Setting $z_{j,i} = d_j$ in **Eq. (29)**, the solutions of adjacent sublayers within the same part as follows.

$$\begin{cases} S_{j,i}(d_j) = T_j(d_j)S_{j,i}(0) + \Phi_{j,i}(d_j) \\ S_{j,i+1}(d_j) = T_j(d_j)S_{j,i+1}(0) + \Phi_{j,i+1}(d_j) \end{cases} \quad (30)$$

The continuity condition between the sublayers is

$$S_{j,i}(d_j) = S_{j,i+1}(0) \quad (31)$$

Perform **Eq. (30)** and **(31)** successively for all the sublayers, and finally the relationship between the state vectors of the lower surface of the j -th hollow cylinder $S_{j,N_j}(d_j)$ and the upper surface $S_{j,1}(0)$ can be expressed as the following formula:

$$S_{j,N_j}(d_j) = [T_j(d_j)]^{N_j} S_{j,1}(0) + \pi_{j,N_j}(d_j), \quad (j=1,2) \quad (32)$$

Where

$$\begin{aligned} \pi_{j,N_j}(d_j) = & [T_j(d_j)]^{N_j-1} \Phi_{j,1}(d_j) + \dots + [T_j(d_j)]^2 \Phi_{j,N_j-2}(d_j) \\ & + T_j(d_j) \Phi_{j,N_j-1}(d_j) + \Phi_{j,N_j}(d_j) \end{aligned} \quad (33)$$

In the local coordinate system of each sublayer, the state vector is

$$S_{j,i}(z_{j,i}) = [U_m^{(j,i)}(z_{j,i}) \quad W_m^{(j,i)}(z_{j,i}) \quad R_m^{(j,i)}(z_{j,i}) \quad Z_m^{(j,i)}(z_{j,i})]^T \quad (34)$$

where $z_{j,i} = 0$ denots sublayer's upper surface, $z_{j,i} = d_j$ denots sublayer's lower surface.

According to the boundary condition **(4)**, the following is given:

$$R_m^{(1,1)}(0) = 0 \quad (35)$$

In addition, the distributed pressure $p(r)$ is known, so $-p(r)$ can be expressed as the form of Fourier-Bessel series according to **Eq. (30)**

$$-p(r) = Z_0^{(1,1)}(0) + \sum_{m=1}^{\infty} Z_m^{(1,1)}(0) V_0(a_m r) \quad (36)$$

According to the boundary condition **(5)**, the following is given:

$$U_m^{(2,N_2)}(d_2) = W_m^{(2,N_2)}(d_2) = 0 \quad (37)$$

According to the boundary condition **(6)**, the following is given:

$$W_m^{(1,N_1)}(d_1) = W_m^{(2,1)}(0), \quad Z_m^{(1,N_1)}(d_1) = Z_m^{(2,1)}(0), \quad R_m^{(1,N_1)}(d_1) = R_m^{(2,1)}(0) = 0 \quad (38)$$

Regarding the variables of $S_{j,N_j}(d_j)$ and $S_{j,1}(0)$ ($j=1,2$) in **Eq. (33)** as unknown, there are 16 unknown variables in total, eight of which can be eliminated by **Eq. (35) ~ (38)**. Therefore, the expression of other unknown variables can be solved from **Eq. (32)**. Obviously, the expression of $S_{j,1}(0)$ is also obtained. It is important to note that the expression of $S_{j,1}(0)$ also contains the undetermined constants $x_{j,i}$ ($i=1,2,\dots,N_j+1$; $j=1,2$). After determining the expression of $S_{j,1}(0)$, by repeating the derivation process of **Eq. (32)**, the stress/displacement of the i -th sublayer in the j -th hollow cylinder can be calculated, matrix $\Pi_{j,i}(z_{j,i})$ and vector $\pi_{j,i}(z_{j,i})$ are not difficultly to obtain.

$$S_{j,i}(z_{j,i}) = \Pi_{j,i}(z_{j,i}) S_{j,1}(0) + \pi_{j,i}(z_{j,i}) \quad (39)$$

If global coordinate z locates in the i -th sublayer of the j -th hollow cylinder, $z_{j,i}$ is given by

$$z_{j,i} = \begin{cases} z - (i-1)d_1, & (j=1) \\ z - h_1 - (i-1)d_2, & (j=2) \end{cases} \quad (40)$$

3.5 Coefficients of Fourier-Bessel Series for $m=0$

The following formulas is obtained from **Eq. (25)** and **(26)**:

$$\begin{cases} Z_0^{(j,i)}(z_{j,i}) = Z_0^{(j,i)}(0) = Z_0^{(1,1)}(0) \\ W_0^{(j,i)}(z_{j,i}) = W_0^{(j,i)}(0) + C_4 Z_0^{(j,i)}(0) z_{j,i} + C_1 (x_{j,i} + x_{j,i+1}) z_{j,i} \end{cases} \quad (41)$$

Particularly, setting $z_{j,i} = d_j$, the following formulas can be obtained:

$$W_0^{(j,i)}(0) = W_0^{(j,i)}(d_j) - C_4 Z_0^{(1,1)}(0) d_j - C_1 (x_{j,i} + x_{j,i+1}) d_j \quad (42)$$

According to the boundary conditions, the following is given:

$$\begin{aligned} W_0^{(2,N_2)}(d_2) &= 0 \\ W_0^{(2,1)}(d_2) &= W_0^{(1,N_1)}(d_1) \\ W_0^{(j,i+1)}(0) &= W_0^{(j,i)}(d_j) \end{aligned}$$

Therefore, all of the $W_0^{(j,i)}(0)$ can be solved from **Eq. (42)**, and then the expression of $W_0^{(j,i)}(z_{j,i})$ at any position can be obtained from **Eq. (41)**.

3.6 Solving the Undetermined Constants

There are $N_j + 1$ undetermined constants $x_{j,i}$ in the j -th hollow cylinder, add up to $N_1 + N_2 + 2$ undetermined constants in hollow cylinder I and II, to solve the undetermined constants, $N_1 + N_2 + 2$ equations were needed. Set $N_1 = 2n_1$, $N_2 = 2n_2$, where n_1, n_2 are positive integer. By solving **Eq. (26)**, **(39)**, **(40)** and **(41)**, $\tilde{U}_{j,i}(z)$, $U_m^{(j,i)}(z)$ and $Z_m^{(j,i)}(z)$ at the position of **Eq. (43)** can be determined, and substituting them into **Eq. (15)** and **(16)**, $N_1 + N_2 + 2$ linear equations are obtained, and all the undetermined constants can be solved. The state variables at any position in the two hollow cylinders can be determined according to **Eq. (39)** and **(41)**, and the corresponding stress/displacement can be obtained by substituting the coefficients into **Eq. (13)**.

$$z = \begin{cases} 2k_1 d_1, & (k_1 = 0, 1, 2, 3, \dots, n_1) \\ 2k_2 d_2, & (k_2 = 0, 1, 2, 3, \dots, n_2, \text{ but } k_2 \neq n_2 - 1) \end{cases} \quad (43)$$

4. Calculation Example

4.1 Comparison of Three Methods

To verify the effectiveness of the above method, a specific example is designed, as shown in **Fig. 4**, the contact stress of the joint surface is extracted, and comparing with the experimental measurement and the finite element analysis result is carried out.

Both the material of the two hollow cylinders are Q235, Young's modulus $E_1 = E_2 = 2 \times 10^5$ MPa, Poisson's ratio $\nu_1 = \nu_2 = 0.3$. the parameters in **Fig. 1** are $a = 6.3\text{mm}$, $b = 45\text{mm}$, $c = 12\text{mm}$, $h_1 = 10\text{mm}$, $h_2 = 20\text{mm}$. The normal load on the surface

is $F = 4500N$, which can be expanded into the form of Fourier-Bessel series according to **Eq. (36)**. The coefficients is given by

$$Z_m^{(1,1)}(0) = \begin{cases} -\frac{c^2 - a^2}{b^2 - a^2} p, & (m = 0) \\ -\frac{pcV_1(\alpha_m c)}{\alpha_m M_m}, & (m = 1, 2, 3, \dots) \end{cases}$$

A satisfactory results was obtained by setting $N_1 = N_2 = 80$ and selecting first 10 items of the Fourier-Bessel series.

In the experimental, two hollow cylinders of Q235 with $\phi 12.6$ through-hole were placed on worktable and connected by M12 bolt and $\phi 24$ gasket. The normal load reached $4500N$, which was measured by a pressure sensor. The contact stress was measured by means of the pressure-sensitive film, as shown in **Fig. 4**.

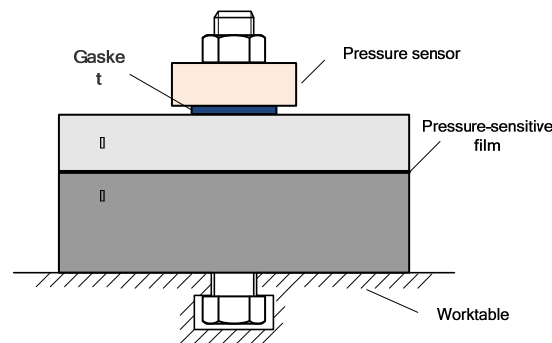
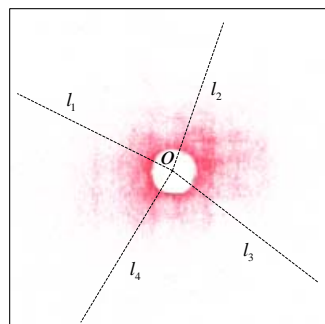
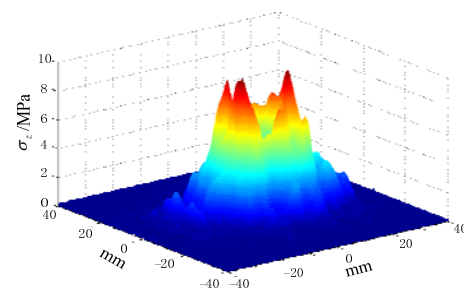


Fig. 4 Experimental setup for joint contact stress test

The white pressure-sensitive film turns red under pressure, and the red concentration increases with the increase of intensity of pressure. So the contact stress can be measured by evaluating the color concentration of the film. **Fig. 5(a)** shows the scanning image of the pressure-sensitive film after experiment. **Fig. 5(b)** shows the contact stress distribution with a three-dimensional figure. The figure clearly shows that the contact stress presents "steep peak" shape distribution, the maximum contact stress appears near the center of the load, and the stress decreases rapidly from the center to the edge until reduces to zero.



(a) Scanning image of the film



(b) 3-D distribution figure

Fig. 5 Contact stress distribution in bolted joint

As shown in **Fig. 5**, because of the machining error of specimens, the position deviation of bolt installation and the measurement error of pressure-sensitive film, measurement result is not absolutely axisymmetric. In order to eliminate the impact of these factors on the measurement result, four straight paths along radial direction, $l_1 \sim l_4$, are set up on the film, as shown in **Fig. 5(a)**. The pressure value of several points of the paths are extracted, and the average value of the same radial position are obtained. Thus, the contact stress distribution along radial direction are obtained. It should be noted that because the measurement error is large near the edge of the hole, the experimental data at the position isn't extracted.

Fig. 6 shows the contact stress distribution curves of state space method (SSM), experimental measurement and finite element method (FEM). The negative value denotes compressive stress. It can be seen that three distribution curves have a good consistency, so the state space method of this paper is accurate and reliable.

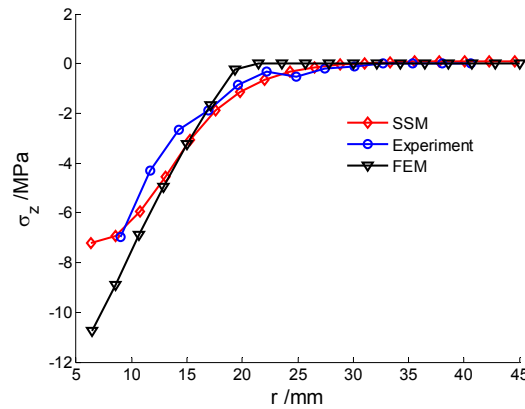
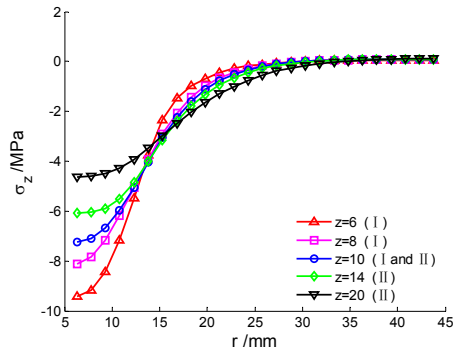


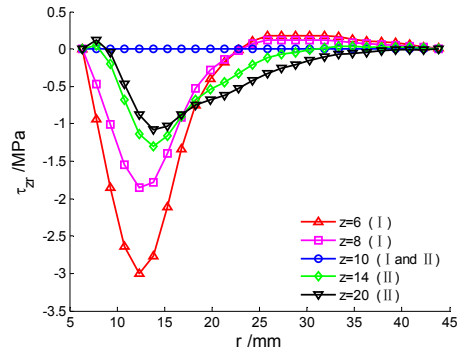
Fig. 6 Data comparison of contact stress

4.2 Stress / Displacement Field in Bolted Joint

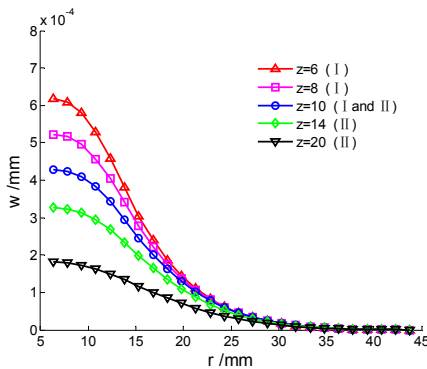
The stress and displacement information of bolted joint are extracted on the basis of the state space method calculate model proposed in this paper. Some stress and displacement distribution curves along radial direction are shown in **Fig. 7**. It can be seen that normal stress σ_z and vertical displacement w both own considerable variation gradient at $r = c$, but tangential stress τ_{rz} and horizontal displacement u appear to be bigger values at $r = c$ than other positions. Moreover, with the increase of coordinate r , all the stresses and displacements tend to zero as shown in **Fig. 7**.



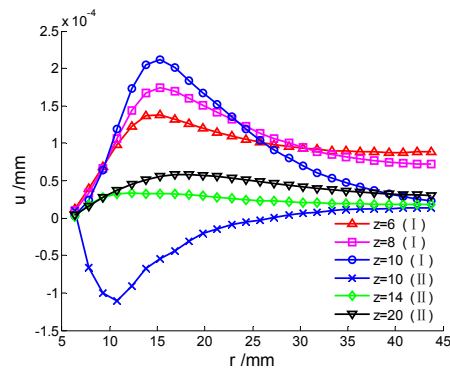
(a) Normal stress σ_z



(b) Tangential stress τ_{zr}



(c) Vertical displacement w



(d) Horizontal displacement u

Fig. 7 Stress and displacement distribution curves along radial direction

For mechanical discontinuous structure problem, normal stress σ_z and vertical displacement w are likely to be the mechanics characteristics people pay more attention to. Some stress and displacement distribution curves along z direction are shown in Fig. 8. It can be seen that σ_z and w decrease nonlinearly with the increase of z . In order to display the distribution of bolted joint under the normal load more visually, the contour map of σ_z and w are drawn, as shown in Fig. 9. The σ_z and w in the bolted joint subjected to a normal load, can transmit swimmingly from the upper plate to the lower plate, and shows a good continuity. The influence region of the external load is mainly on the surface region $a \leq r \leq c$, as well as its lower region. With the increase of z , the influence region spreads gradually, nevertheless, the stress and displacement decrease rapidly.

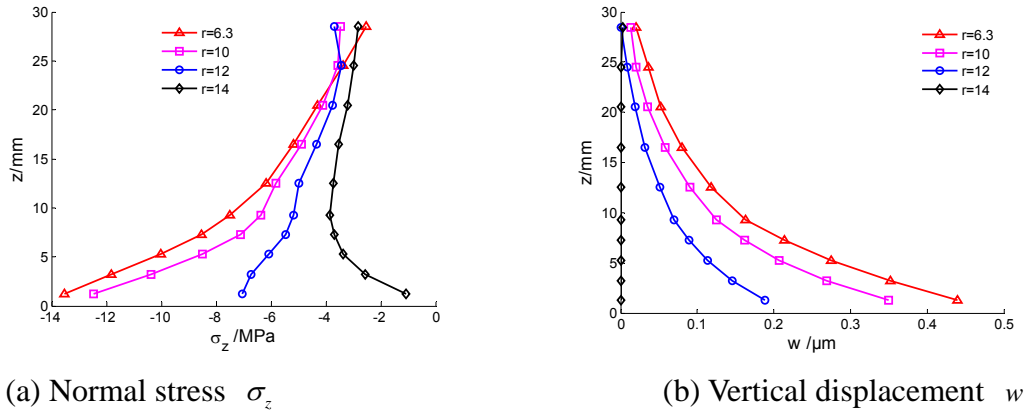


Fig. 8 σ_z and w distribution curves along z direction

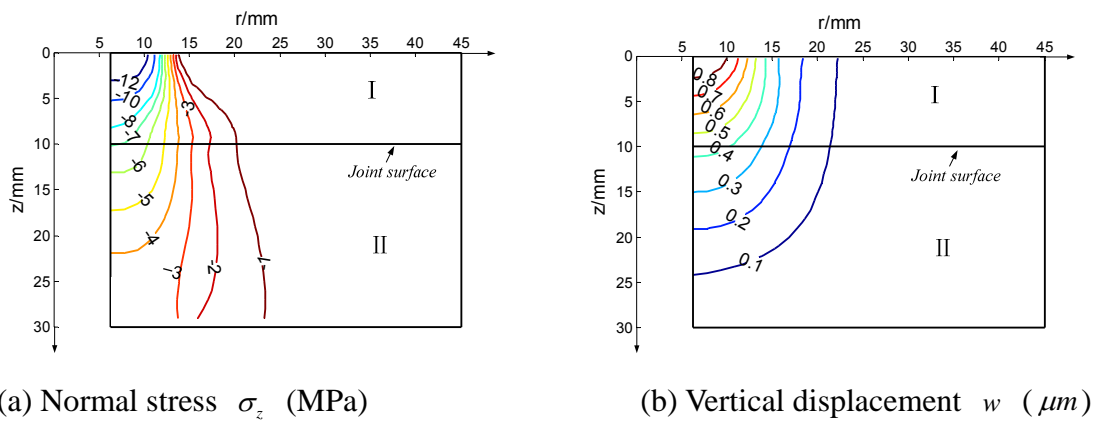


Fig. 9 Contour map of σ_z and w

5. Conclusions

A stress/displacement field calculation model combining elastic mechanics with state space theory is established to solve the mechanical calculation problem associated with the discontinuity of structure and material in bolted joints. The stress / displacement distribution regularities of the joint surface and the components are obtained accurately, and the transfer characteristic of mechanics characteristics in bolted joint structure is analyzed.

The calculation model based on state space theory is a new way to calculate the stress / displacement field in bolted joints rapidly. It can rapidly and accurately obtain the relationship between the mechanics characteristics distributions in bolted joint and the factors such as structure, material, load, and so on, and has a wide application prospect in the design and optimization process of bolted joints.

This model still has some shortcomings. For example, because of ignoring the flatness, waviness and roughness of the contact surfaces, there will be a deviation between the calculation results and the actual situation to some extent. The object of the model is only limited to simple geometric shapes and force conditions. The analytical model of the mechanics characteristics of the complex geometry parts subjected to non-axisymmetric loads or horizontal load (unidirectional load, rotational load) needs further study.

Acknowledgement

This work supported by National Natural Science Foundation of China(No.51475077,51005038) and Science and Technology Foundation of Liaoning, China (No.201301002, 2014028012).

References

- [1] Honglin Z, Qingxin D, Ming Z, et al. Theoretic analysis on and application of behaviors of machine tool joints[J]. Chinese Journal of Mechanical Engineering, 2008, 44(12): 208-214.
- [2] Nassar S A, Abboud A. An improved stiffness model for bolted joints[J]. Journal of Mechanical Design, 2009, 131(12): 121001.
- [3] Mi L, Yin G, Sun M, et al. Effects of preloads on joints on dynamic stiffness of a whole machine tool structure[J]. Journal of Mechanical Science and Technology, 2012, 26(2): 495-508.
- [4] Benhamena A, Talha A, Benseddiq N, et al. Effect of clamping force on fretting fatigue behaviour of bolted assemblies: Case of couple steel–aluminium[J]. Materials Science and Engineering: A, 2010, 527(23): 6413-6421.
- [5] Tian H, Li B, Liu H, et al. A new method of virtual material hypothesis-based dynamic modeling on fixed joint interface in machine tools[J]. International Journal of Machine Tools and Manufacture, 2011, 51(3): 239-249.
- [6] Wang L, Du R, Jin T, et al. Matching Design for Bolted Joints Based by Effective Contact Radius Maximization[J]. Journal of Xi'an Jiaotong University, 2013, 7: 013.
- [7] Namazi M, Altintas Y, Abe T, et al. Modeling and identification of tool holder–spindle interface dynamics[J]. International Journal of Machine Tools and Manufacture, 2007, 47(9): 1333-1341.
- [8] Singhal V, Litke P J, Black A F, et al. An experimentally validated thermo-mechanical model for the prediction of thermal contact conductance[J]. International Journal of Heat and Mass Transfer, 2005, 48(25): 5446-5459.
- [9] Voller G P, Tirovic M. Conductive heat transfer across a bolted automotive joint and the influence of interface conditioning[J]. International Journal of Heat and Mass Transfer, 2007, 50(23): 4833-4844.
- [10] Chandrashekhara K, Muthanna S K. Analysis of a thick plate with a circular hole resting on a smooth rigid bed and subjected to axisymmetric normal load[J]. Acta Mechanica, 1979, 33(1-2): 33-44.
- [11] Sawa T, Kumano H, Kobayashi F, et al. On the characteristics of bolted joints with gaskets: stress analysis of a metal flat gasket interposed between two hollow cylinders[J]. Bulletin of JSME, 1984, 27(227): 900-908.
- [12] Sawa T, Kumano H, Morohoshi T. The contact stress in a bolted joint with a threaded bolt[J]. Experimental Mechanics, 1996, 36(1): 17-23.
- [13] Gray P J, McCarthy C T. A global bolted joint model for finite element analysis of load distributions in multi-bolt composite joints[J]. Composites Part B: Engineering, 2010, 41(4): 317-325.
- [14] Guo Y, Parker R G. Stiffness matrix calculation of rolling element bearings using a finite element/contact mechanics model[J]. Mechanism and Machine Theory, 2012, 51: 32-45.
- [15] Sethuraman R, Kumar T S. Finite element based member stiffness evaluation of axisymmetric bolted joints[J]. Journal of Mechanical Design, 2009, 131(1): 011012.

- [16] Li S. Finite element analyses for contact strength and bending strength of a pair of spur gears with machining errors, assembly errors and tooth modifications[J]. Mechanism and Machine Theory, 2007, 42(1): 88-114.
- [17] Xiang Y, Wang C M. Exact buckling and vibration solutions for stepped rectangular plates[J]. Journal of sound and Vibration, 2002, 250(3): 503-517.
- [18] Chen W Q, Ding H J. On free vibration of a functionally graded piezoelectric rectangular plate[J]. Acta Mechanica, 2002, 153(3-4): 207-216.
- [19] Ying J, Lü C F, Chen W Q. Two-dimensional elasticity solutions for functionally graded beams resting on elastic foundations[J]. Composite Structures, 2008, 84(3): 209-219.
- [20] Hongyu S, Jiarang F. Axisymmetric bending for thick laminated circular plate under a concentrated load[J]. Applied Mathematics and Mechanics, 2000, 21(1): 95-102.
- [21] Hongyu S. Analytical solution of bending problem for thick laminated circular plate on elastic foundation with free edges[J]. Chinese Journal of Geotechnical Engineering, 2000, 3: 011.